

- (11) P. J. Flory, "Statistical Mechanics of Chain Molecules", Interscience, New York, 1969.
- (12) J. G. Kirkwood and J. Riseman, *J. Chem. Phys.*, **16**, 565 (1948); P. L. Auer and C. S. Gardner, *ibid.*, **23**, 1545 (1955).
- (13) P. J. Flory and T. G. Fox, Jr., *J. Am. Chem. Soc.*, **73**, 1904 (1951).
- (14) W. H. Stockmayer and M. Fixman, *J. Polym. Sci., Part C*, **1**, 137 (1963).
- (15) H. Inagaki, H. Suzuki, and M. Kurata, *J. Polym. Sci., Part C*, **15**, 409 (1966).
- (16) M. Bohdanecký, *Collect. Czech. Chem. Commun.*, **30**, 1576 (1965).
- (17) J. M. G. Cowie, *Polymer*, **7**, 487 (1966).
- (18) P. Mark and S. Windwer, *J. Chem. Phys.*, **47**, 708 (1967).
- (19) P. Munk and M. E. Halbrook, *Macromolecules*, **9**, 568 (1976).
- (20) S. G. Chu and P. Munk, *J. Polym. Sci., Polym. Phys. Ed.*, **15**, 1163 (1977).
- (21) S. G. Chu and P. Munk, *Macromolecules*, **11**, 101 (1978).
- (22) M. Nakata, S. Higashida, N. Kuwahara, S. Saeki, and M. Kaneko, *J. Chem. Phys.*, **64**, 1022 (1976).
- (23) G. Meyerhoff, *Z. Phys. Chem. (Frankfurt am Main)*, **4**, 335 (1955).
- (24) G. C. Berry, *J. Chem. Phys.*, **44**, 4550 (1966).
- (25) H. Inagaki, H. Suzuki, M. Fujii, and T. Matsuo, *J. Phys. Chem.*, **70**, 1718 (1966).
- (26) M. Fukuda, M. Fukutomi, Y. Kato, and T. Hashimoto, *J. Polym. Sci., Polym. Phys. Ed.*, **12**, 871 (1974).
- (27) B. Nyström and J. Roots, *Eur. Polym. J.*, **14**, 551 (1978).
- (28) D. Y. Yoon, P. R. Sundararajan, and P. J. Flory, *Macromolecules*, **8**, 776 (1975).
- (29) D. Lath and M. Bohdanecký, *J. Polym. Sci., Polym. Lett. Ed.*, **15**, 555 (1977).
- (30) N. Kuwahara, S. Saeki, S. Konno, and M. Kaneko, *Polymer*, **15**, 66 (1974).
- (31) S. Konno, S. Saeki, N. Kuwahara, M. Nakata, and M. Kaneko, *Macromolecules*, **8**, 799 (1975).
- (32) J. E. Mark and P. J. Flory, *J. Am. Chem. Soc.*, **87**, 1423 (1965).
- (33) J. Biroš, L. Zeman, and D. Patterson, *Macromolecules*, **4**, 30 (1971).

Solid State Extrusion of Poly(vinylidene fluoride).

1. Ram and Hydrostatic Extrusion

W. T. Mead, Anagnostis E. Zachariades, Toshio Shimada, and Roger S. Porter*

Polymer Science and Engineering Department, Materials Research Laboratory, University of Massachusetts, Amherst, Massachusetts 01003. Received September 11, 1978

ABSTRACT: Oriented films and fibers of poly(vinylidene fluoride) have been prepared by solid state extrusion and hydrostatic extrusion to an extrusion draw ratio of 8. The properties of the fibers and films have been assessed by several techniques including infrared spectroscopy, thermal analysis, and X-ray. A maximum birefringence of 0.039, a modulus of 3.5 GPa, a melting point increase of 5 °C, and a crystallinity of 50% were obtained for the extrudates. Shrinkage of fibers observed along the chain orientation axis is possibly due to retractive forces of the deformed noncrystalline phase. Infrared bands of the α - and β -polymorphic phases showed that extrusion produced a conversion from the α to the β phase.

The solid state extrusion of polyethylene¹ and the higher Nylons² has produced ultraoriented morphologies. Enhanced tensile moduli up to 70 GPa have been obtained for polyethylene which is approximately one-fourth of the theoretical crystal modulus for its orthorhombic unit cell.³⁻⁷ The theoretical crystal modulus for poly(vinylidene fluoride), PVF₂, in the chain direction has been shown to be 235 GPa, a value comparable with those for the higher Nylons⁸ and polyethylene. Solid state extrusion of PVF₂ might also be expected to produce an ultraoriented fiber with high modulus. Further interest for extrusion of PVF₂, apart from the potential of producing a high modulus morphology, however, is due to its pronounced potential piezo- and pyroelectric activity.

PVF₂ can exist in three crystalline conformations:^{9,10} phase I (or β form) has a planar zig-zag structure; phase II (or α form) has a sequence of approximately alternating gauche and trans bonds. The existence of a third phase was first suggested by Natta, et al.¹¹ Cortili and Zerbi^{12,13} and Gal'Perrin et al.¹⁴ have described the preparation and characteristics of this third polymorph, phase III (γ form). Lando and Doll¹⁰ and others¹⁵ speculate on the conformation of phase III as planar zig-zag, based on the similarity of infrared spectra between forms I and III.

The crystallites of the β form exhibit a permanent polarization. The relative amounts of α and β forms reportedly depend on the draw temperature and draw ratio. Lando and Doll¹⁰ showed that PVF₂ films conventionally drawn at 50 °C produced only the β form, whereas drawing above 100 °C increased the α form content. The solid state

extrusion temperature should therefore be at least 50 °C below the PVF₂ ambient melting point (~170 °C) with the limitation of ever decreasing extrusion rates at lower temperatures.⁵ Solid state extrusion has produced polyethylene extrudates with near perfect crystal orientation and with a birefringence greater than the intrinsic birefringence of the single crystal.⁶ It is thus anticipated that the method may provide a possible route for obtaining increased pyroelectricity and/or piezoelectric activity for ultraoriented PVF₂, since Glass et al.¹⁶ have reported a correlation between birefringence and pyroelectricity of PVF₂.

Kolbeck and Uhlmann,¹⁷ using the method of extrusion reported by Southern and Porter,¹⁸ have independently shown that solid state extrusion of PVF₂ is possible.

In the present paper, preliminary experiments on ram and hydrostatic extrusion of PVF₂ are presented, and the resulting filament and film properties are analyzed using the techniques discussed elsewhere.⁵⁻⁷

Experimental Section

Materials. The Pennwalt Corp. Kynar series 301, 450, and 820 were used having cited melting points of 156, 155, and 166 °C, respectively. A further sample, a copolymer of vinylidene fluoride and tetrafluoroethylene (73% CH₂CF₂, 27% C₂F₄), Kynar 7201 (not available commercially), was supplied kindly by Dr. G. T. Davis and Dr. M. Broadhurst of the U.S. National Bureau of Standards.

Extrusion. Poly(vinylidene fluoride) was oriented by solid state extrusion procedures described elsewhere.¹⁹ Briefly the PVF₂ was isothermally crystallized under high pressure (0.23 GPa). The

melting point of PVF₂ increases with pressure about 3.3×10^{-7} K/Pa¹⁰ and hence 0.23 GPa applied pressure increases the melting point of PVF₂ by $\sim 76^\circ\text{C}$. The PVF₂ was crystallized at $\sim 160^\circ\text{C}$ for 30 min and subsequently extruded to a length L , through a stainless steel conical die of included angle $2\theta = 20^\circ$, exit radius $r = 6.6 \times 10^{-4}$ m, and maximum extrusion draw ratio of 52. The extrusion draw ratio of the fiber when $L > 1$ is¹⁹

$$\text{EDR}(\theta, L) \approx \left(\frac{3L \tan \theta}{r} \right)^{2/3} \quad \text{for } 1 < \text{EDR}(\theta, L) < 5 \quad (1)$$

Thin films required for infrared studies were obtained by solid state extrusion through wedge-shaped or slit dies. The extrusion draw ratio of the single-angle wedge-shaped die may be expressed by

$$\text{EDR} = [1 + (4L/t) \tan \theta]^{1/2} \quad \text{for } 1 < \text{EDR} < 2b/t \quad (2)$$

$2b$ is the maximum inset width of the die, L is the extrusion length, θ is the semiangle of the die, and t is the slit width, equal to the film thickness. The stainless steel die used had dimensions $b = 3 \times 10^{-2}$ m, $\theta = 6.8^\circ$, and $t = 50 \times 10^{-4}$. This valuation of EDR as a function of fiber length represents an approximation since it is assumed that elongation and no shear flow occur.¹⁷

The method of extrusion used was similar to that first reported by Southern and Porter¹⁸ for HDPE and by Kolbeck and Uhlmann¹⁷ for PVF₂ extrusion. The PVF₂ extrudates were readily produced by crystallizing the polymer melt by forcing it through a capillary die at constant velocity at extrusion temperatures above the ambient melting point. For example, Kynar 820 readily extruded at 176°C , 11°C above its ambient melting point at a pressure of 0.23 GPa where the polymer is crystallizing. However, extrusion at temperatures below the ambient melting point of PVF₂ produced a rapid decrease in extrusion rate for all the extrusion methods discussed above. The low rates for solid billet extrusion of PVF₂ were partially overcome by using a hydrostatic procedure; the only difference from the conventional method was that a lubricant (STP) was used to transmit the applied pressure to the PVF₂ billet and constant velocity of the piston was maintained, as in the original method of Southern and Porter.¹⁸

Characterization. Melting points and crystalline fractions were determined using a Perkin-Elmer DSC-1B operating at a $10^\circ\text{C min}^{-1}$ heating rate. Linear thermal expansion coefficients and length variations with temperature were determined using a Perkin-Elmer Thermomechanical Analyzer. Birefringence measurements were obtained using an Ehringhaus Calcite Rotary compensator with a Zeiss polarizing microscope and white light source. Wide- and small-angle X-ray diffraction patterns were recorded with a Warhus camera using Ni-filtered Cu K α radiation (35 kV, 20 mA). Tensile measurements were determined at room temperature using Instron TTM and a 2.5×10^{-3} m strain gauge extensometer. Further details of these techniques are described elsewhere.^{5,6} Infrared spectra of the extruded films were recorded in the infrared region $400\text{--}1000\text{ cm}^{-1}$ using the Perkin-Elmer 289 spectrophotometer.

Results and Discussion

Extrusion Rate. The extrusion rate of PVF₂ from the conical die was measured as a function of draw ratio or fiber length, L , and used to calculate an apparent elongational viscosity $\eta_E = \sigma_z/\dot{\gamma}$ where the elongation rate, $\dot{\gamma} = 1/L (dL/dt)$ and σ_z , the axial stress, are assumed equal to the applied pressure. Figure 1 shows the variation of η_E with draw ratio, temperature and pressure for Kynar 820 crystallized at 164°C and 0.23 GPa and extruded at 0.23 GPa and 0.49 GPa (dotted line).

The initial low value of η_E with extrusion draw ratio, EDR, for HDPE⁵ has been attributed to the deformation of the original spherulitic morphology producing transparency at the tip of the conical die.⁵ The apparent elongational viscosity rapidly increases at draw ratios greater than 7 and the high value of $d\eta_E/d(\text{DR})$ would suggest that the natural draw ratio of the polymer is 7–8. Continuous lengths of extruded PVF₂ were obtained at high extrusion rates ($\sim 5\text{ cm min}^{-1}$) by extrusion at

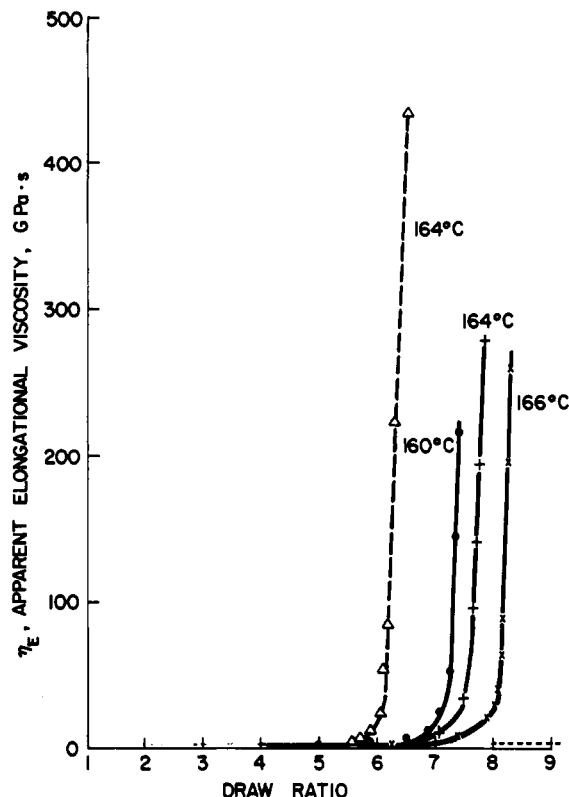


Figure 1. Variation of apparent elongational viscosity with draw ratio for Kynar 820 crystallized at 164°C (0.23 GPa) and conventionally extruded at 0.23 GPa and at temperatures as shown. Dotted line for extrusion pressure 0.49 GPa.

temperatures near their ambient melting point and using dies with maximum draw ratio less than 7 since the rapid strain hardening does not then occur as shown in Figure 1.

According to Figure 1, higher extrusion temperatures result in higher draw ratios prior to strain hardening, as defined by the rapid increase of apparent elongational viscosity with draw ratio. Such behavior is similar to that reported by Mead, Desper, and Porter⁶ for HDPE. With decreasing extrusion temperature the crystallinity, crystalline perfection, and orientation of HDPE decreased and the noncrystalline phase readily oriented as strain hardening occurred at low draw ratios.⁶ The rapid increase of the apparent elongational viscosity with draw ratio was associated with the strain hardening and orientation of the interlamellar region which increased with applied strain and/or lower temperatures. Poly(vinylidene fluoride), which only has a maximum crystallinity of $<50\%$, should therefore rapidly strain harden as the noncrystalline phase is oriented.

An apparent activation energy for deformation for PVF₂ may be obtained⁵ by plotting the logarithm of η_E at a given draw ratio as a function of the inverse of the absolute extrusion temperature. For PVF₂, η_E was measured only for $160\text{--}166^\circ\text{C}$. At a draw ratio of 7 an apparent activation energy of deformation for PVF₂ of 570 kJ mol^{-1} (137 kcal mol^{-1}) is estimated using the data from the small temperature range of Figure 1.

To overcome the slow extrusion rates and high apparent elongational viscosities obtained in solid state extrusion, possibly due to an increase in the frictional coefficient between polymer and die, hydrostatic extrusion was used. Initial extrusion rates were too high to measure for the hydrostatic extrusion of precrystallized PVF₂ at 2400 atm (0.23 GPa) and 10°C below the ambient melting point at a constant plunger velocity of 0.5 cm min^{-1} . The pressure

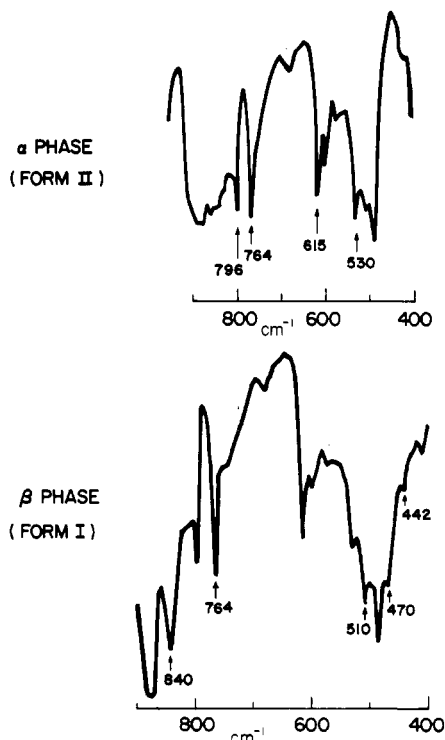


Figure 2. Infrared spectra for PVF₂ films of Kynar 301: (a) lightly pressed thin film, (b) extrudate, crystallized and hydrostatically extruded at 155 °C and 0.23 GPa through the slit die, draw ratio of 4.

rapidly increased, corresponding to an unsteady state condition, and then approached a constant value. The maximum pressure was $\sim 1/8$ of that required in the conventional extrusion using 0.23 GPa.

The variation of η with draw ratio for PVF₂ extruded at 0.49 GPa is shown in Figure 1 (dotted line). Increasing the extrusion pressure from 0.23 to 0.49 GPa produces strain hardening at lower draw ratios. This is possibly because of the compressibility of PVF₂, since at 20 °C the specific volume of α and β forms decreases by $\sim 8.2 \times 10^{-6} \text{ m}^3 \text{ kg}^{-1}$,²¹ as the pressure is increased from 0.24 to 0.49 GPa. Indeed, dilatometry for phase α ¹⁰ at two different pressures (0.04 and 0.15 GPa) shows a marked decrease in specific volume at temperatures near the ambient melting point. The formation of the β form during extrusion might be related to the decrease of extrusion rate with draw ratio. The transformation from α to β phase for PVF₂ is expected to increase as the extrusion temperature is lowered, consistent with decreasing extrusion rates. Peterlin and Elwell²⁸ note that the β transition peak in PVF₂ relates to rotation of chain sections in the non-crystalline regions outside the lattice and its intensity is strongly reduced by chain orientation. The shift of the absorption maxima of the β peak to lower frequencies and higher temperature was attributed to increased interchain interaction due to alignment and closer packing and this might explain the variation of extrusion rate with formation of the β phase. Further considerations of the pressure dependence for flow concern the effect of die angle on extrusion characteristics. Nakayama and Kanetsuna²² found that low die angles facilitate extrusion of polyethylene free from cracks. Predecki and Statton²³ and Perkins and Porter,^{2,24} have used low die angles to extrude the higher Nylons. Stallings and Howell²⁵ have also noted that entrance angles of dies should be less than 15° for efficient extrusion of PVF₂ in the melt state. The following paper²⁶ will discuss a coextrusion method which enables films to be extruded at high rates.

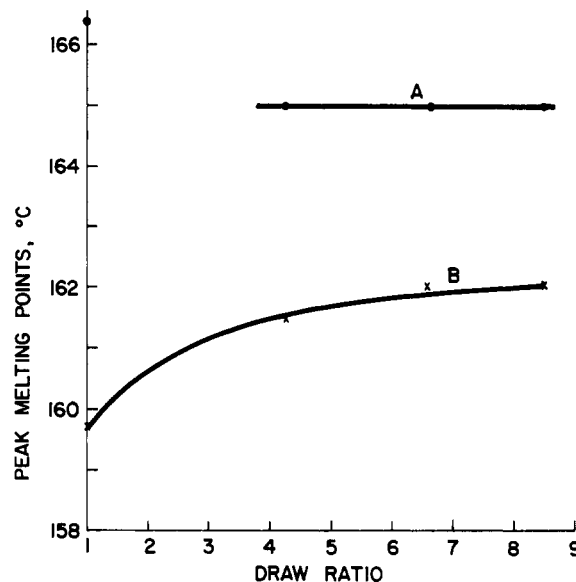


Figure 3. Double melting endotherm peaks A and B for hydrostatically extruded PVF₂, $M_w = 35000$ (Kynar 820), crystallized at 164 °C (0.23 GPa) and extruded at 140 °C and 0.23 GPa.

Infrared Analysis. Figure 2 shows the IR spectra of PVF₂ (Kynar 301) obtained before and after solid state hydrostatic extrusion. The unextruded PVF₂ consists of the α form, i.e., phase II. IR absorption bands observed at 530, 615, 764, and 796 cm^{-1} are characteristic of the TGTG' conformation of the α form.²⁷ After extrusion, new bands at 442, 470, 510, and 840 cm^{-1} are observed,²⁶ characteristic of the planar zig-zag conformation of the β form. Small peaks at 530, 615, 764, and 796 remain indicating that a small amount of the α form is still present in the extrudate.

An attempt was also made to produce oriented γ form PVF₂ by extrusion. According to Hasegawa et al.,⁹ the γ form of PVF₂ is obtained by application of 5000 atm (0.49 GPa) at 250 °C for 1 h. On cooling the billet to 155 °C and extruding at 0.49 GPa, oriented β form was obtained. IR spectra for the γ modification show absorption bands at 430 and 481 cm^{-1} ,¹²⁻¹⁴ whereas those for the β form occurred at 442, 470, and 484 cm^{-1} . Similar observations have been made by Hasegawa⁹ et al. who attempted to produce an oriented form of γ modification by rolling films of PVF₂.

Thermal Analysis. Heats of fusion, melting points, and shrinkage measurements of PVF₂ extrudates are discussed briefly in this section. The heat of fusion of the as-received Kynar 301 was 30.5 J g⁻¹ and had a peak melting point of 150 ± 1 °C at 10 °C min⁻¹ heating rates. Fibers prepared by solid state extrusion at 157 °C and 0.23 GPa for an isothermally crystallized morphology of Kynar 301 at 157 °C and 0.23 GPa had a heat of fusion of 39.8 J g⁻¹ (at EDR = 1) and increased slightly to 41.4 J g⁻¹ at a draw ratio of 4. These correspond to crystallinities of 38.8 and 40.5% assuming a mean value for ΔH_c , the heat of fusion of the crystalline PVF₂, given as 100.2²⁹ and 104.8³⁰ J g⁻¹, i.e., 102.5 J g⁻¹. This heat of fusion is also assumed to be the same for all forms of PVF₂ even though the crystalline density of the β form has been cited as $1.90 \times 10^3 \text{ Kg m}^{-3}$ while the density of the α form at 20 °C is reportedly 1.77 Kg m^{-3} .¹⁰

Figure 3 shows the variation of the two peak melting points of Kynar 820 $M_w = 35 \times 10^3$ crystallized at 164 °C and 0.23 GPa and extruded at 140 °C and 0.23 GPa. The melting point increase of ~ 2 °C for the low-melting endotherm of PVF₂ suggests that chain extension does not

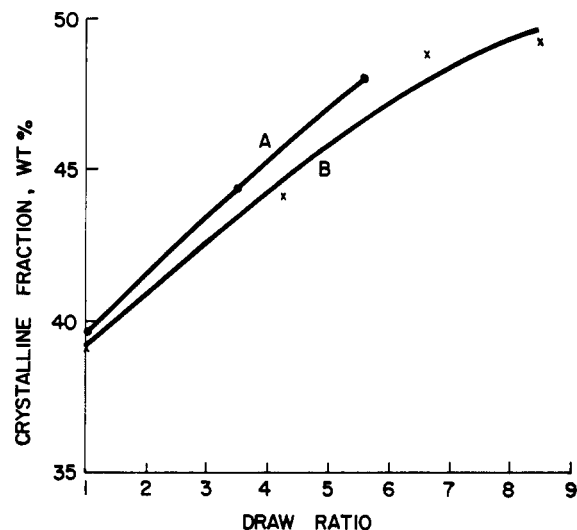


Figure 4. Variation of melting endotherms with draw ratio of solid state conventionally extruded PVF₂ (Kynar 7201). Crystallization and extrusion at 124 °C and 0.23 GPa.

readily occur as for extruded HDPE, where a melting point increase of ~5 °C and a crystallinity of ~85% are obtained.

Crystallization of Kynar 450 at 250 °C and 0.49 GPa also produced two melting endotherms at 158 and 188 °C using a 10 °C min⁻¹ DSC heating rate.

The melting behavior of the as-received Kynar 7201 consisted of two melting peaks at 112 and 118 °C. The recrystallized billet at atmospheric pressure had two melting peaks at 122 and 137 °C and heat of fusion 26.3 J g⁻¹. An increase in the heat of fusion to 40.6 J g⁻¹ occurred on crystallization at 124 °C and 0.23 GPa. Upon solid state extrusion to EDR ~5 the heat of fusion increased to 41.5 J g⁻¹.

Crystallization of Kynar 450 at 250 °C and 0.49 GPa also produced two melting endotherms at 125 and 137 °C using a 10 °C min⁻¹ DSC heating rate. The relative areas of the two peaks subsequently varied with extrusion draw ratio as shown in Figure 4. Several explanations for the multiple melting endotherm of PVF₂ may be possible. Nakagawa and Ishida³⁰ studied the annealing of the α form at different temperatures. Quench crystallized and annealed and quenched samples both showed two endothermic peaks. The lower peak was attributed to melting of crystals originally present. High-temperature annealing of quenched PVF₂ produces α form crystals with a bimodal distribution of lamellar thickness. Prest and Luca²⁷ have shown that the rapid crystallization produces an unstable morphology composed of α form which at slow heating rates will recrystallize to produce a higher melting species of α form.

In summary of the preliminary DSC data presented for extruded PVF₂ fibers, two melting endotherms are usually observed, and it is the lower peak which increases in area and melting point with draw ratio. At present, however, the DSC data do not allow unambiguous interpretation of the nature of the crystalline phases and possible correlation of the conversion of the α to the β phase with the infrared data is discussed in the Infrared Analysis section. A more detailed discussion of DSC data of extruded PVF₂ is presented in another article.²⁶

The reversible linear thermal expansion coefficient for the extruded Kynar 301 fiber at room temperature and draw ratio of unity was $\sim 1.3 \times 10^{-5} \text{ }^\circ\text{C}^{-1}$, as deduced from Figure 6 which shows fractional fiber length (L) changes ($\Delta L/L$) on warming PVF₂ fibers from -100 °C.

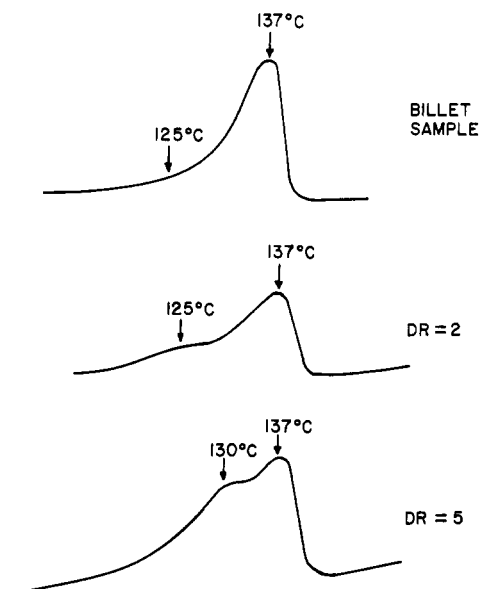


Figure 5. Variation of crystallinity with draw ratio of Kynar 820 crystallized at 164 °C (0.23 GPa) and extruded: 160 °C, 0.23 GPa using a stainless steel die with a maximum draw ratio of 52; hydrostatic extrusion at 140 °C at 0.5 cm min⁻¹ plunger velocity.

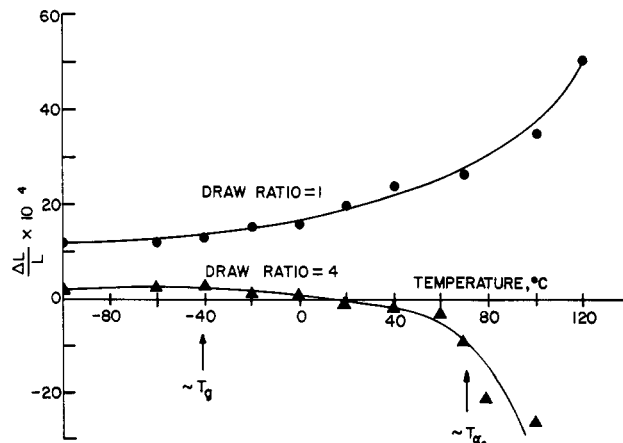


Figure 6. Change in fractional length with temperature for solid state conventionally extruded PVF₂ (Kynar 301). Crystallization and extrusion at 155 °C and 0.23 GPa.

At a draw ratio of unity the fiber length rapidly expands ~30 °C below its melting point of 150 °C and extrusion temperature 160 °C. On warming the unoriented PVF₂ from -100 °C, $\Delta L/L$ appears to first change with temperature near -50 °C. The T_g for PVF₂ is located near -40 °C according to dilatometric data³¹ as well as thermally stimulated current measurements from polarized PVF₂.³²

The extruded PVF₂ fiber has a negative expansion coefficient when warmed above -40 °C, corresponding to contraction of the fiber along its extrusion axis. A negative expansion coefficient is obtained at room temperature for the extruded fiber and these data suggest that the PVF₂ extruded fibers readily creep, anneal, and lose their orientation at room temperature. Crystallinity of the extruded PVF₂ fiber increased by only 10%, as discussed above, yet the extrusion produced a change of sign of its expansion coefficient. It is possible, therefore, that the negative expansion coefficient for PVF₂, or decrease in the positive linear expansion coefficient with draw ratio, is due to retractive forces produced by increased orientation of the noncrystalline phase at high draw ratios, since the percent crystallinity is near 50%.

Sasabe et al.,³³ Yano,³⁴ and Kakutani³⁵ have reported the α_c absorption at 70 °C (110 Hz) and related the ab-

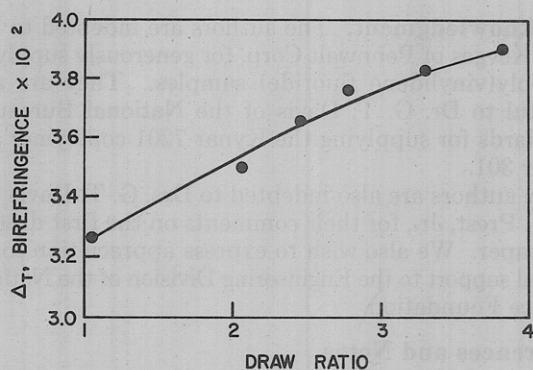


Figure 7. Variation of birefringence with draw ratio of conventionally extruded PVF₂ (Kynar 301) crystallized and extruded at 156 °C (0.23 GPa).

sorption to the molecular motion of the molecules in crystalline regions. An α_2 absorption was also reported by Kakutani³⁵ at 110 °C and was related to the β crystalline form. Rapid contraction of the fiber is observed near 70 °C. However, the negative expansion coefficients obtained from data of Figure 6 are most likely related to the retractive force of the noncrystalline phase, since only positive expansion coefficients are obtained for the α polymorph crystalline phase. For example, in the temperature range 20 to 120 °C, the values of the lattice constants a , b , and c for the unit cell of phase II increase by approximately 1.2, 0.8, and 0.4%, respectively.³⁶ The linear expansion coefficients along the crystallographic axes for the β polymorph do not appear to have been published.

The thermal shrinkage measurements of PVF₂ provide interesting comparison with those for ultraoriented HDPE. Rapid contraction of the HDPE extruded fiber was observed at temperatures greater than 80 °C and below the ambient melting point.⁶ The change of sign of α , the linear expansion coefficient, with draw ratio was cited by Porter et al. as evidence for the HDPE fibers containing a component of chain extended morphology, a continuous crystal, with planar zig-zag packing in an orthorhombic unit cell.³⁷ The expansion coefficient (–120 to –80 °C) of the HDPE fiber at draw ratio ~ 40 approached the crystallographic c axis value of $-12 \times 10^{-6} \text{ }^\circ\text{C}^{-1}$. However, for extruded PVF₂ the linear expansion coefficients of the crystallographic axis are positive even though a negative expansion coefficient is observed for the extruded fiber.

Birefringence. The birefringence variation with draw ratio for Kynar 301 crystallized and conventionally extruded at 156 °C and 0.23 GPa is given in Figure 7. The birefringence increase for the hydrostatically extruded fiber was less efficient with extrusion draw ratio for the conventionally extruded specimen. The possible effect of lubricant plasticizing the polymer might account for such behavior. At high draw ratio the lubricant is unable to penetrate the oriented fiber. A birefringence of 0.032 detected for the extruded fibers at an extrusion draw ratio slightly greater than unity might be due to a small degree of orientation during the crystallization of the performed morphology in the die. The value of 0.039 obtained for the Pennwalt 301 sample extruded to a draw ratio near 4 is greater than the value of 0.035 obtained by Shuford et al.³⁸ by uniaxial deformation of PVF₂ to a draw ratio of 7.

The total birefringence, Δn_T , is a measure of the contributions due to the crystalline phase, the noncrystalline phase, and the form birefringence. The birefringence contribution of the crystalline and noncrystalline phases can be estimated by the equation proposed by Stein in which the extrudate is assumed to consist of two phases.⁶

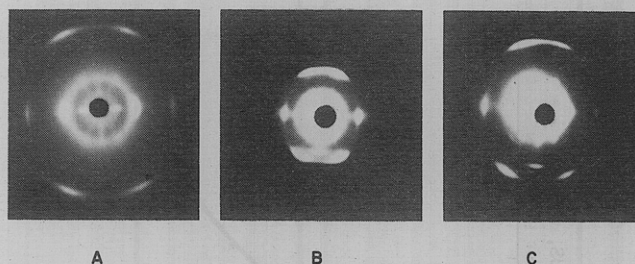


Figure 8. Wide-angle X-ray diffraction patterns of Kynar 450: (a) thin film of as-received PVF₂ lightly pressed between plates at 170 °C and cooled to room temperature; (b) isothermal crystallization and extrusion at 155 °C and 0.23 GPa; and (c) isothermal crystallization for 1 h at 250 °C and 0.49 GPa and subsequent extrusion at 155 °C and 0.49 GPa. The draw ratio is 7 and the fiber axis is vertical.

The intrinsic birefringences of the different conformations and phases do not appear to have been estimated for PVF₂ and are required if the noncrystalline orientation is to be deduced. Birefringence of ultraoriented HDPE approached a maximum value comparable and slightly greater than the theoretical value for the crystal.⁶ Birefringence draw ratio behavior of PVF₂, shown in Figure 7, approaches a limiting value of $\sim 4 \times 10^{-2}$, which is a possible crude estimate of Δ_c° , the intrinsic birefringence of the crystal for PVF₂.

X-ray Studies. Figure 8 shows the wide-angle diffraction patterns of Kynar 450 melt-pressed film and Kynar 450 fibers conventionally extruded to a draw ratio of 7 at 155 °C and 0.23 and 0.49 GPa. The patterns do show some slight asymmetry and are similar to those reported by Hasegawa.⁹

Prior to extrusion, the X-ray pattern shows a mixture of α and β forms with the weak reflections of the β form dominated by those of the α form.

All fibers and films obtained by extrusion of PVF₂ produced an axial long period of approximately 200 Å. Small-angle X-ray scattering showed two maxima elongated perpendicular to the fiber axis, indicating that the lateral dimensions of the crystallites are small. The diffraction pattern shows that the highly oriented fiber structure consists of stacks of folded chain crystallites arranged regularly with the fiber axis. Even at a draw ratio of 7 a two point SAXS pattern for PVF₂ was obtained indicating the predominance of chain folding and incomplete alignment of crystallites with draw direction.

Mechanical Tests. The tensile modulus of the extruded fibers increases with draw ratio, as shown in Figure 9 for Kynar 820. Fibers extruded were not sufficiently long to be clamped for testing. The fiber did not fracture during extrusion in the manner described for polyethylene, although some surface marks were noted at a draw ratio of 8 similar to those described by Buckley and Long.³⁹ The maximum modulus obtainable is only about a percent of the theoretical value for this polymer. The maximum sonic modulus value obtained by Shuford³⁸ was 475 kpsi (3.2 GPa at a draw ratio of 7) which is comparable to the value reported here of 3.2 GPa also at a draw ratio of 7. This modulus is over twice the value of unoriented PVF₂.

The tensile strength obtained from a fiber with draw ratio between 3 and 7 was 38 MPa with strain to break of $\sim 50\%$, as compared with the tensile strength to break of the original isotropic material, quoted by Pennwalt as 5023 ± 256 psi (33 MPa) and elongation to break of $\sim 200\%$.

Conclusions

Poly(vinylidene fluoride) has been solid state and hydrostatically extruded through conical and slit dies to a extrusion draw ratio of 8. Solid state extrusion produced

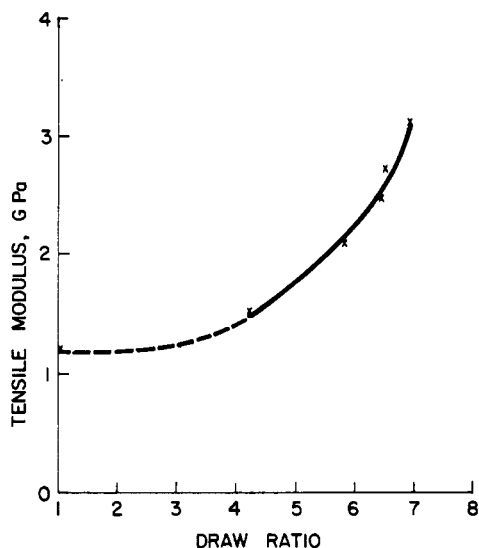


Figure 9. Tensile modulus variation with draw ratio of hydrostatically extruded PVF₂ (Kynar 820) crystallized at 164 °C and 0.23 GPa. Extrusion temperature 140 °C; extrusion plunger velocity 0.5 cm min⁻¹.

high chain orientation of the crystalline phase in the extrusion direction. Extruded PVF₂ fibers exhibit strain hardening corresponding to a rapid decrease in extrusion rate using constant applied pressure, or a rapid increase in the apparent elongational viscosity with draw ratio. On lowering the extrusion temperature below the melting point, η_E approaches values for deformation of glass, and an apparent activation energy of 570 kJ mol⁻¹ was estimated.

In accord with the two modes of apparent elongation viscosity, PVF₂ extrudates exhibit an initially slow and then rapid increase in tensile modulus with a maximum of 3.5 GPa at a draw ratio of 7, as the birefringence attains a maximum of 0.039. Phase transformation in the extrudates from α to β form was detected by IR, thus producing the phase yielding a large dipole moment normal to the chain axis.

The PVF₂ crystallinity was increased by 10% absolute during extrusion and produced two peak endothermic melting points, similar to those obtained by annealing. The phase having the lower melting peak increased its melting point and volume fraction during extrusion. The following paper will discuss the DSC endotherms in more detail.

The difference in extrusion behavior of HDPE and PVF₂ might be attributed to the differences in maximum crystallinity. The relatively low crystallinity in PVF₂ (50%) compared to HDPE extrudate (85%) would indicate that the noncrystalline phase determines the formation characteristics. The extrusion characteristics of PVF₂ were similar to extrusion properties of ultra high molecular weight HDPE.⁵ Further support for this conclusion is obtained from the linear expansion coefficient measurements. Although the linear expansion coefficients of the crystallographic axes of PVF₂ are positive, a negative expansion coefficient is observed for the extruded fiber and would result from the retractive forces of the noncrystalline phase.

In conclusion it appears that solid state extrusion of PVF₂ offers a possible route to maximum piezoelectricity, provided sufficiently low extrusion temperatures are used, high draw ratios are used, and the extrusion rates are sufficiently high.

Acknowledgment. The authors are indebted to Mr. John Kevgas of Pennwalt Corp. for generously supplying the poly(vinylidene fluoride) samples. They are also grateful to Dr. G. T. Davis of the National Bureau of Standards for supplying the Kynar 7201 copolymer and Kynar 301.

The authors are also indebted to Drs. G. T. Davis and W. M. Prest, Jr., for their comments on the first draft of this paper. We also wish to express appreciation for financial support to the Engineering Division of the National Science Foundation.

References and Notes

- (1) C. R. Desper, J. H. Southern, R. D. Ulrich, and R. S. Porter, *J. Appl. Phys.*, **41**, 4284 (1970).
- (2) W. G. Perkins and R. S. Porter, *Bull. Am. Phys. Soc.*, **AJ10**, 235 (1976).
- (3) N. J. Capiati and R. S. Porter, *J. Polym. Sci.*, **13**, 1177 (1975).
- (4) F. C. Frank, *Proc. R. Soc., London Ser. A*, **319**, 127 (1970).
- (5) W. T. Mead and R. S. Porter, *J. Polym. Sci. Polym. Symp.*, accepted.
- (6) W. T. Mead, C. R. Desper, and R. S. Porter, *J. Polym. Sci., Polym. Phys. Ed.*, submitted.
- (7) W. T. Mead and R. S. Porter, "The Influence of Initial Morphology on the Physical and Mechanical Properties of Extruded High Density Polyethylene", Flow Induced Crystallization Symposium, Midland Macromolecular Institute, Mich., August 1977, accepted.
- (8) T. R. Manley and G. G. Martin, *Polymer*, **14**, 491, 632 (1973).
- (9) R. Hasegawa, *Polym. J.*, **3**, 591, 600 (1972).
- (10) J. B. Lando and W. W. Doll, *J. Macromol. Sci., Phys.*, **2**, 205, 219 (1968); **4**, 309, 897 (1970).
- (11) G. Natta, G. Allegra, I. W. Bassi, D. Sianesi, G. Caporioac, and E. Torti, *J. Polym. Sci.*, **3**, 4263 (1965).
- (12) G. Zerbi and G. Cortili, *Chem. Commun.*, **13**, 295 (1965).
- (13) G. Cortili and G. Zerbi, *Spectrochim. Acta, Part A*, **23**, 285 (1967).
- (14) Ye. L. Gal'Perrin, Yu. V. Strogalin, and M. P. Mlenik, *Vysokomol. Soedin.*, **7**, 933 (1965).
- (15) R. Hasegawa, Y. Tanabe, M. Kobayashi, H. Tadokoro, A. Sawaoka, and N. Kawai, *J. Polym. Sci., Polym. Symp.*, **8**, 1073 (1970).
- (16) A. M. Glass, J. H. McFee, and J. G. Bergman, *J. Appl. Phys.*, **42**, 5219 (1971).
- (17) A. G. Kolbeck and D. R. Uhlmann, *J. Polym. Sci.*, **15**, 27 (1977).
- (18) J. H. Southern and R. S. Porter, *J. Macromol. Sci., Phys.*, **4**, 541 (1970).
- (19) N. J. Capiati, S. Kojima, W. G. Perkins, and R. S. Porter, *J. Mater. Sci.*, **12**, 334 (1977).
- (20) W. T. Mead and R. S. Porter, *J. Appl. Polym. Sci.*, accepted.
- (21) J. B. Lando, H. G. Olf, and A. Peterlin, *J. Polym. Sci., Part A*, **4**, 941 (1966).
- (22) K. Nakayama and H. Kanetsuna, *Kobunshi Ronbunshu*, **31**, 256 (1974).
- (23) P. Predecki and W. O. Statton, *J. Polym. Sci., Polym. Lett. Ed.*, **10**, 87 (1972).
- (24) W. G. Perkins, Ph.D. Thesis, University of Massachusetts, 1978, unpublished.
- (25) J. P. Stallings and S. G. Howell, *Polym. Eng. Sci.*, **11**, 507 (1971).
- (26) T. Shimada, A. E. Zachariades, W. T. Mead, and R. S. Porter, *J. Cryst. Phys.*, accepted.
- (27) W. M. Prest, Jr., and J. Luca, *J. Appl. Phys.*, **46**, 4136 (1975).
- (28) A. Peterlin and J. H. Elwell, *J. Mater. Sci.*, **2**, 1 (1967).
- (29) T. Suwa, T. Seguchi, K. Makuuchi, T. Abe, N. Tamura, and M. Takehisa, *Nippon Kagaku Kaishi*, **5**, 1046 (1973).
- (30) K. Nakagawa and Y. Ishida, *J. Polym. Sci.*, **11**, 2153 (1973).
- (31) L. Mandelkern, G. M. Martin, and F. A. Quinn, *J. Res. Natl. Bur. Stand.*, **58**, 2745 (1957).
- (32) G. Pfister and M. A. Abkowitz, *J. Appl. Phys.*, **45**, 1001 (1974).
- (33) H. Sasabe, S. Saito, M. Asahina, and H. Kakutani, *J. Polym. Sci., Polym. Symp.*, **7**, 1405 (1969).
- (34) S. Yano, *J. Polym. Sci., Polym. Symp.*, **8**, 1057 (1970).
- (35) H. Kakutani, *J. Polym. Sci., Polym. Symp.*, **8**, 1177 (1970).
- (36) K. Nakagawa and Y. Ishida, *Kolloid Z. Z. Polym.*, **251**, 103 (1973).
- (37) R. S. Porter, N. W. Weeks, N. J. Capiati, and R. J. Krzewski, *J. Therm. Anal.*, **8**, 547 (1975).
- (38) R. J. Shuford, A. F. Wilde, J. J. Ricca, and G. R. Thomas, *Polym. Eng. Sci.*, **16**, 25 (1976).
- (39) A. Buckley and H. A. Long, *Polym. Eng. Sci.*, **9**, 115 (1969).